Resource

Cell Chemical Biology

A Rapid and Precise Mutation-Activated Fluorescence Reporter for Analyzing Acute Mutagenesis Frequency

Graphical Abstract

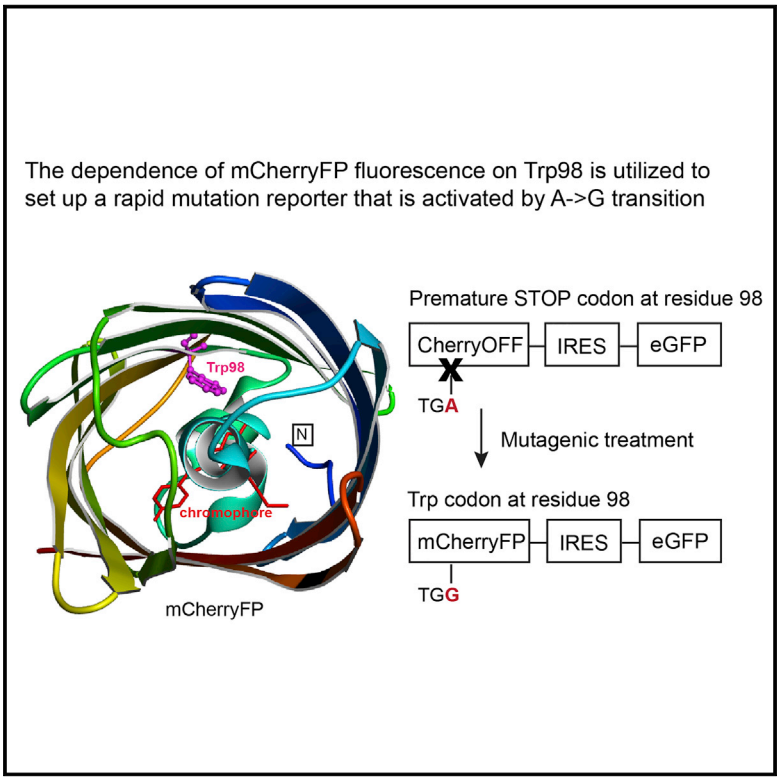

Highlights

- Mutation-activated fluorescence of CherryOFF quickly reports mutation frequencies
- Point mutations (A/T–G/C) are detected with high precision and accuracy
- CherryOFF-GFP is not limited by cell lines, stresses, or reagents
- CherryOFF can be adapted to detect other point mutations and indels

Authors

Michael D. Birnbaum, Leah Nemzow, Akhilesh Kumar, Feng Gong, Fangliang Zhang

Correspondence

fgong@med.miami.edu (F.G.), fzhang2@miami.edu (F.Z.)

In Brief

The mutation-activated CherryOFF-GFP reporter quickly and accurately reflects point mutation frequency via flow cytometry readout. This reporter can easily be adapted for different point mutations and indels.

Birnbaum et al., 2018, Cell Chemical Biology *25*, 1–12
August 16, 2018
https://doi.org/10.1016/j.chembiol.2018.05.010

CellPress

Please cite this article in press as: Birnbaum et al., A Rapid and Precise Mutation-Activated Fluorescence Reporter for Analyzing Acute Mutagenesis Frequency, Cell Chemical Biology (2018), https://doi.org/10.1016/j.chembiol.2018.05.010

Cell Chemical Biology
Resource

A Rapid and Precise Mutation-Activated Fluorescence Reporter for Analyzing Acute Mutagenesis Frequency

Michael D. Birnbaum,[1] Leah Nemzow,[2] Akhilesh Kumar,[1,4] Feng Gong,[2,3,*] and Fangliang Zhang[1,3,5,*]
[1]Department of Molecular & Cellular Pharmacology, University of Miami, Miami, FL 33136, USA
[2]Department of Biochemistry & Molecular Biology, University of Miami, Miami, FL 33136, USA
[3]Sylvester Comprehensive Cancer Center, University of Miami, Miami, FL 33136, USA
[4]Present address: Department of Botany, Banaras Hindu University, Varanasi 221005, India
[5]Lead Contact
*Correspondence: fgong@med.miami.edu (F.G.), fzhang2@miami.edu (F.Z.)
https://doi.org/10.1016/j.chembiol.2018.05.010

SUMMARY

Mutagenesis reporters are critical for quantifying genome stability. However, current methods rely on cell survival/death to report mutation, which takes weeks and prevents evaluation of acute or time-dependent changes. Existing methods also have other limitations, such as cell type restrictions. Using our discovery that mCherryFP fluorescence depends on residue Trp98, we replaced this codon with a stop codon to generate a mutation biosensor (termed CherryOFF), with a green fluorescence protein (GFP) as an internal control. We found that the red fluorescence of this biosensor is activated by a specific A/T-G/C nucleotide transition. Compared with the established hypoxanthine phosphoribosyl transferase assay, our reporter has similar or better ability to detect changes of mutation frequency induced by physical/chemical mutagens or manipulation of mutation-related genes. Furthermore, CherryOFF-GFP can report mutagenesis independently of cell-death events, can be adapted to many cell types, and can generate readouts within 1 day for the measurement of acute or time-dependent events.

INTRODUCTION

Genomic mutations are the driving force for molecular evolution and are also directly linked to cancer and many other diseases. Mutations are mainly induced by infidelities in DNA replication or DNA damage by stressors such as ultraviolet (UV) light and genotoxic/mutagenic chemical agents. As a defense mechanism against DNA damage, normal cells possess DNA repair, cell cycle checkpoint, and other genome-stabilizing mechanisms that reduce mutation frequency. Therefore, measuring the genomic mutation frequency provides first-hand evidence regarding the physiological state of a cell, is important for investigating the roles of any genetic or epigenetic factors in genomic stability, and is essential for evaluating the mutagenic/genotoxic effects of stressors. As such, tools for measuring mutation frequency are of fundamental significance for studies of basic mechanisms and diseases such as cancer.

Many reporter systems have been developed to indirectly quantify the level of genomic mutation frequency in simple organisms, such as the Ames test for bacteria (Mortelmans and Zeiger, 2000) and the canavanine resistance assay for yeast (Shor et al., 2013). However, fewer options exist for mammalian cells. One of the most popular assays for mammalian systems utilizes hypoxanthine phosphorybosyl transferase (HPRT), whose enzymatic activity is needed to fully propagate the cytotoxic effects of nucleoside analog 6-thioguanine (6-TG). As such, spontaneous mutations that inactivate HPRT allow cell growth in the presence of 6-TG. A relative of the hypoxanthine phosphoribosyl transferase (HPRT) assay is the xanthine-guanine phosphoribosyl transferase (XPRT) assay, which utilizes a transgenic Chinese hamster ovary cell line lacking HPRT and the transduction of a single copy of *Escherichia coli* XPRT to confer sensitivity to 6-TG. A more recently developed assay, the mouse lymphoma assay (MLA), utilizes mouse lymphoma L5178Y cells to detect mutations at the thymidine kinase (Tk) locus via sensitivity to trifluorothymidine (Gad, 2008). All of the above three methods are endorsed by the Organisation for Economic Co-operation and Development guidelines for evaluating genotoxicity (Johnson, 2012). However, these assays rely on cell death to distinguish non-mutant from mutant cells, thus taking several days or even several weeks for outputs. In addition, many factors are known to affect the cellular sensitivity (dose response) to cytotoxin 6-TG, either by attenuating the apoptosis pressure or by affecting metabolic pathways that detoxify 6-TG (such as thiopurine methyltransferase) (Dean, 2012; Gefen et al., 2010; Ichikawa et al., 2000). This may create difficulty for investigating genes that have dual roles in mutation and cell death/survival/metabolism, which include many cancer-related genes such as P53 and PTEN (Giono and Manfredi, 2006; Song et al., 2012; Vogelstein et al., 2000). Furthermore, all the above traditional methods have cell type limitations. The XPRT and MLA assays are performed in specific cell lines. While the HPRT assay is more flexible with cell types, it still requires colony formation of the cells for accurate readout. Finally, due to the requirement of long incubation periods, none of these existing assays for mammalian cells is capable of monitoring acute or time-dependent events in mutagenesis.

More recently, assays utilizing fluorescence proteins as genetically encoded biosensors for mutagenesis have avoided the usage of cytotoxic reagents. In most of these methods, the fluorescent signals are constantly active unless being deactivated by mutation (Fu et al., 2015). However, assays based on readouts on negative selection (loss of signal) usually suffer from high levels of noise, which reduce their ability to detect small changes with sufficient statistical confidence. In addition, the loss of fluorescent signal may be induced by many processes other than mutations, including spontaneous gene silencing. To achieve better ability in detection, a more favorable approach is to generate a gain of fluorescence as a readout signal. Such strategies have been employed in a small number of recent studies to report the activity of DNA-modifying enzymes or for tracing cell lineage (Ma et al., 2016; Ro, 2004; Tichy et al., 2011). However, a mutation-activated reporter has not been adapted to measure global mutation frequency.

Recently, when we looked to measure the effects of arginyltransferase 1 (Ate1) on mutation frequencies in mouse embryonic fibroblasts (MEF), we found that this measurement cannot be readily accomplished with the currently available mutation reporter assays. For this reason, we designed a mutation reporter in which the mCherryFP gene is disrupted by replacing a Trp codon (TGG) at residue 98 with a premature stop codon (TGA). Under the assumption that any new mutation changing the premature stop codon to a sense codon would re-activate the red fluorescence, we found that this mutation reporter was able to detect the effect of ATE1-knockout on the mutation frequency in UV-irradiated MEFs (Kumar et al., 2016). However, the mechanism and property of this reporter remain poorly characterized. In particular, it remains unknown what mechanism leads to the activation of the fluorescence, what types of mutation are detected in this assay, and how this assay compares with traditional tools in terms of accuracy, specificity, versatility, and other benchmarks.

In this report, we describe in detail the mechanism, setup, and the application of this gain-of-function mutation-activated fluorescence reporter, termed CherryOFF-GFP. We further showed this reporter was suitable for measuring mutation levels under different conditions and has a very low false-positive rate and a very fast turnover time. We demonstrated this reporter is suitable for measuring acute and time-dependent mutagenesis. Furthermore, this assay can reliably measure and compare mutation frequencies in different types of cells regardless of their colony-forming ability or tolerance to cellular stressors.

RESULTS

The Mechanism of CherryOFF-GFP Reporter Is Based on the Trp98 Dependency for mCherryFP Fluorescence

The CherryOFF-GFP reporter was constructed by placing two fluorescence proteins, mCherryFP and GFP, under the same promoter and separated with an internal ribosome entry site (IRES) (Figure 1A). We replaced a single nucleotide in the coding sequence of mCherryFP, which mutates the codon for Trp98 residue (TGG) into a premature termination codon TGA (Figure 1A). The resulting protein is not expected to have fluorescence. However, if a single-nucleotide transition of A to G on the sense strand, or T to C on the antisense strand (referred as A/T to G/C hereafter) takes place at that codon, this reverting mutation will allow a functional mCherryFP to be expressed. It is important to point out that Trp98 is not part of the known chromophore core of mCherryFP, which consists of the tri-peptide Met-Tyr-Gly at residues 71–73 (Shaner et al., 2004). However, our structural analysis (Figure 1B) revealed that Trp98 (Figure 1B, pink highlight) locates inside the barrel-like chamber of mCherryFP and is spatially not far away from the tri-peptide chromophore core (Figure 1B, red highlight) (Bekker et al., 2016). As such, it is possible this bulky, hydrophobic, and intrinsically fluorescent Trp98 residue is required for the microenvironment of a functional chromophore in mCherryFP. However, besides a reverting event to restore the Trp residue, other unique single-nucleotide mutations may take place at the codon corresponding to residue 98, which are expected to result in either a different stop codon, or five other amino acids: glycine, serine, leucine, cysteine, and arginine (Figure 1C). To understand what type of nucleotide mutation event is detected by this mutation reporter, it is important to understand the consequence of these other amino acids on the fluorescent signal of the mCherryFP protein. For this reason, variants of mCherryFP with mutations replacing residue 98 with glycine, serine, leucine, cysteine, or arginine were constructed and expressed, compared with positive and negative controls of the wild-type (WT) mCherryFP and Cherry-OFF-GFP. We found that only the cells carrying the WT Trp98 had red fluorescence (Figure 1D). These results confirm that the Trp98 residue is essential for mCherryFP's fluorescent signal. Therefore, the mutation reporter CherryOFF-GFP as demonstrated here specifically tests A/T to G/C transition mutations.

The CherryOFF-GFP Mutation-Activated Reporter Can Detect Changes in Mutation Frequency with an Ability Comparable with the HPRT Assay

To ensure the fidelity of this reporter before applying it, several control experiments were done to establish gating. After standard forward and side scatter gating to remove cell debris or aggregates (Figure S1B), the gating for detection of red fluorescence was established by comparing the fluorescence profile of a negative control cell line that only expresses green fluorescence protein (GFP) and a positive control that expresses both red fluorescence protein and GFP (Figure 2A). Please see additional details in the STAR Methods for suggested guidelines and discussions for the gating setup.

To test whether our mutation-activated reporter is suitable for measuring mutation burden in cells, we first compared its performance with a known and published use of the classic, gold-standard HPRT assay. In a previously published report (Zhang et al., 2015b), the HPRT assay was used to show that downregulation of ubiquitin-specific peptidase 24 (*USP24*) leads to a significant increase of spontaneous mutation in HCT116 cells, an aggressive yet slowly motile cancer cell line that tends to form colonies in culture. In our study, we repeated this experiment to directly compare the performance of the HPRT assay and the CherryOFF-GFP reporter. Consistent with the results from the HPRT assay, readouts from the CherryOFF-GFP assay indicated higher numbers of red cells in *USP24* knockdown (KD) cells compared with the control HCT116 cells, although the statistical significance obtained by the CherryOFF-GFP is higher than the HPRT assay (Figures 2B and 2C). To further validate the ability

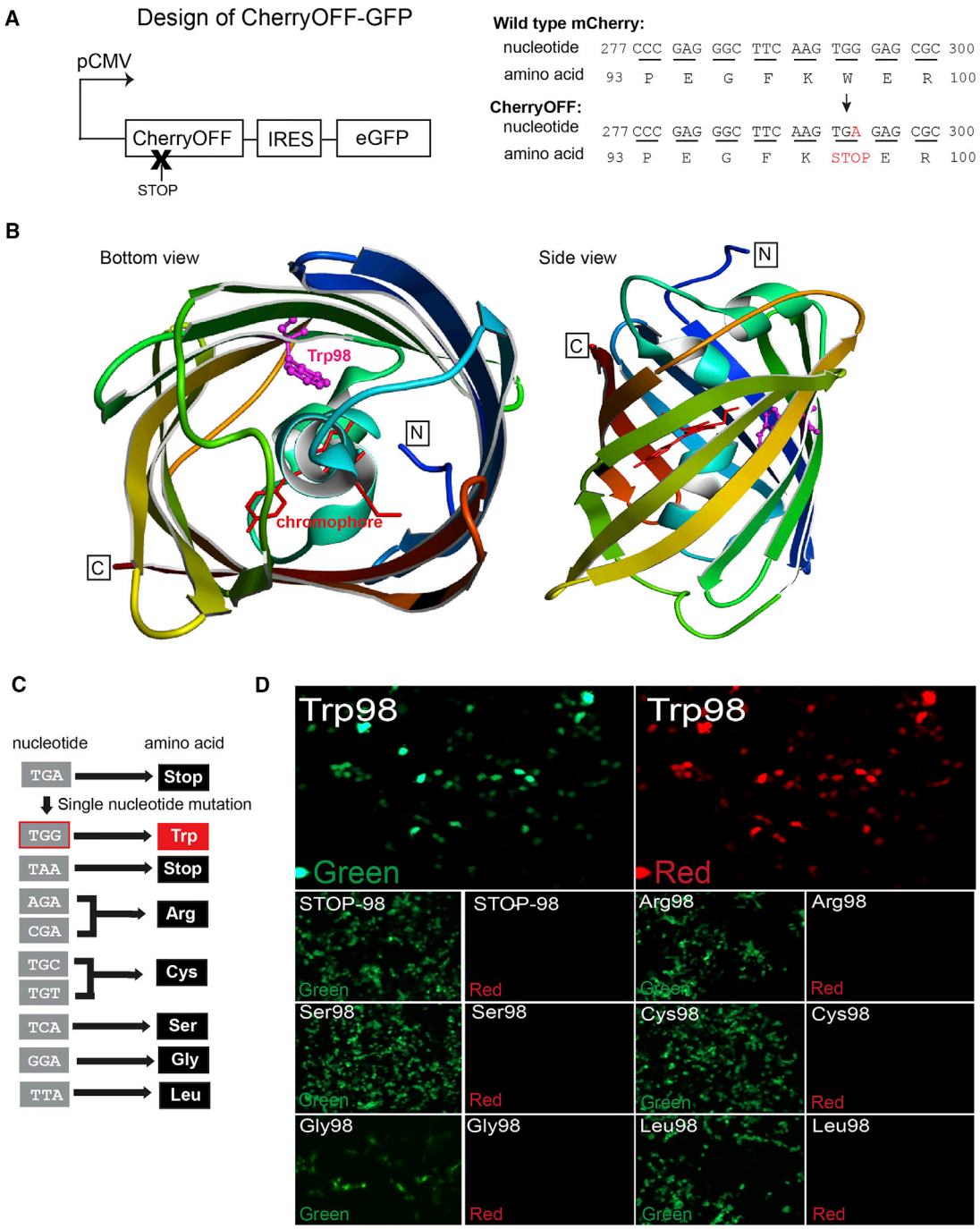

Figure 1. Construction of CherryOFF-GFP Reporter via Loss-of-Function Point Mutation at Trp98 Codon

(A) Left: a schematic of CherryOFF-GFP vector. An internal ribosomal entry site (IRES) separates nonfunctional mCherryFP and functional GFP, driven by the cytomegalovirus promoter. Right: site-directed G-to-A point mutation of mCherryFP's coding sequence at Trp98 creates a premature stop codon TGA.

(B) Bottom view and side view of three-dimensional structure of mCherryFP shows the Trp98 residue (pink) pointing inward toward the chromophore (red) at the center of the protein.

(C) Schematic of possible single point mutations at TGA codon of residue 98. Besides a reversion to the Trp codon (TGG), other point mutations may result in arginine, cysteine, glycine, leucine, serine, or another stop codon TAA.

(D) mCherryFP constructs carrying Trp98, Stop-98, and the five other possible revertant amino acids at residue 98 were expressed in HEK 293T cells. Detectable red fluorescence was only found in Trp98-mCherryFP, suggesting that Trp98 is essential for the red fluorescence signal, and therefore only an A/T to G/C reversion in CherryOFF-GFP can restore the fluorescent signal.

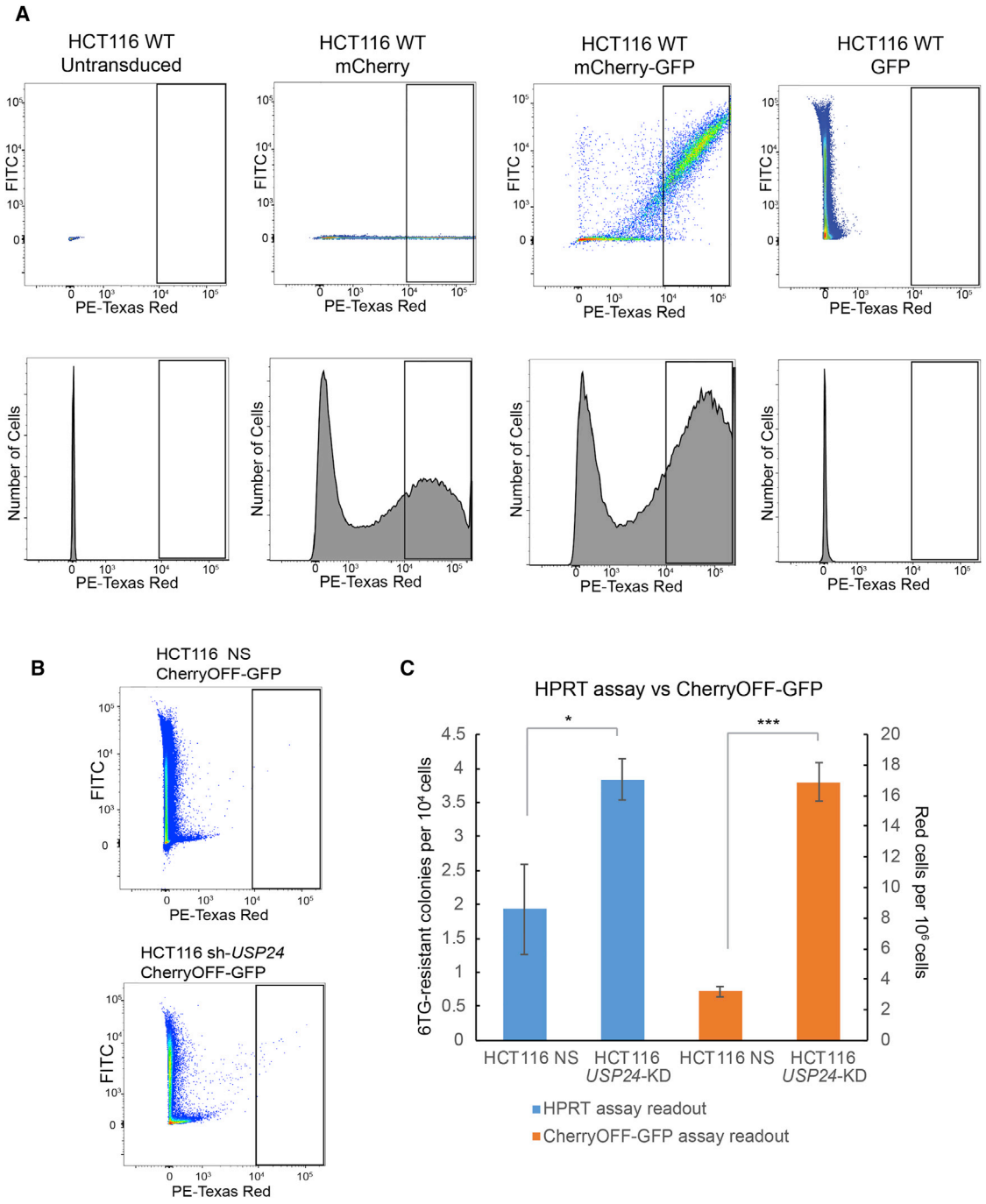

Figure 2. The Setup of CherryOFF-GFP Reporter and Its Comparison with HPRT Assay in a Known Mutagenic Context

(A) Two-dimensional (green-red) distribution chart and the corresponding red fluorescence signal histograms from flow cytometry for HCT116 cells that either express GFP or mCherryFP individually, both, or neither. The gating thresholds were chosen to exclude any negative cells while covering the vast majority of the cells expressing mCherryFP. See Figure S1A for additional information for the viral copy numbers in the transduced cells. See also Figures S1B, S1C, and S2 for the setup of gating with HCT cells and MEF cells, respectively. See also Figure S4 for additional information for the impact of threshold changes on analysis results.

(B) HCT116 colon cancer cells carrying CherryOFF-GFP and small hairpin RNA (shRNA) targeting *USP24* or nonsilencing (NS) control. See Figure S3B for *USP24* KD efficiency. Representative flow diagrams of these cells show a small fraction of positive red events in the cells with NS shRNA, and a higher signal in the *USP24* KD cells.

(legend continued on next page)

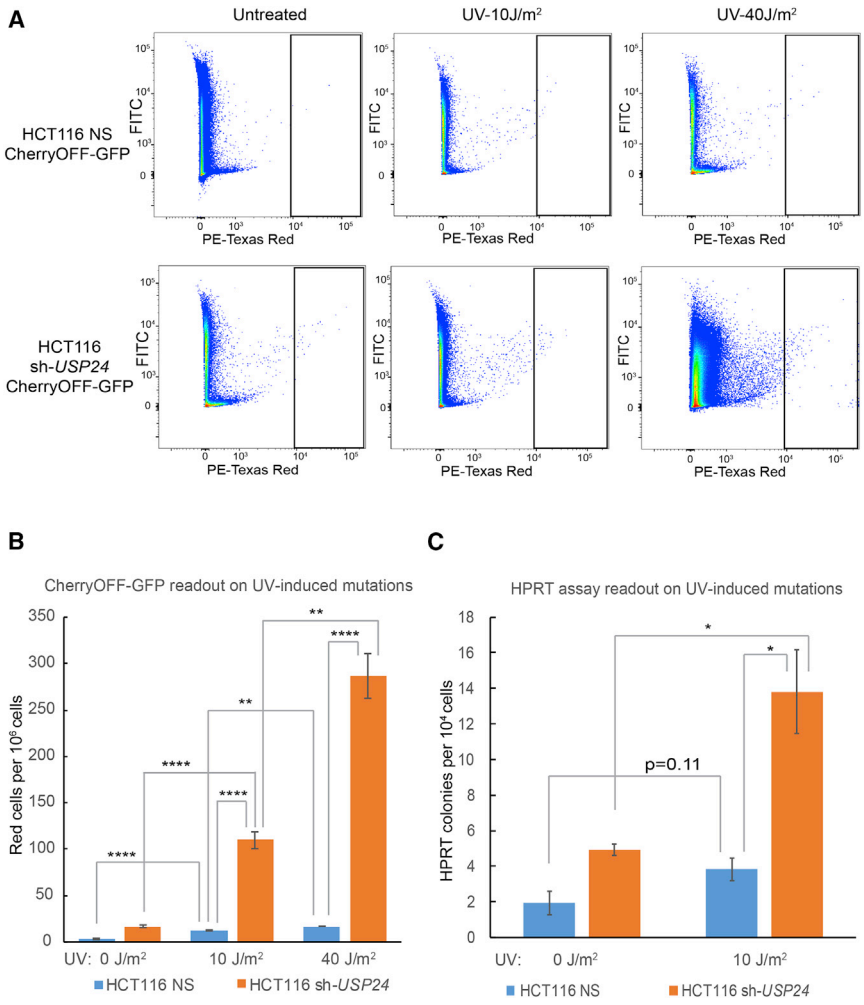

Figure 3. CherryOFF-GFP Compared with HPRT to Assess UV-Driven Mutagenesis in HCT116 Cells With or Without *USP24* KD

(A) Representative red-green flow diagrams of HCT116 cells carrying CherryOFF-GFP and *USP24* KD or nonsilencing shRNA control, exposed to 10 or 40 J/m^2 UV radiation, or untreated. UV irradiation increased mutagenesis in both cell lines, and higher mutagenesis was seen in *USP24* KD.

(B) Quantification of (A).

(C) HPRT assay was performed with the same conditions as CherryOFF-GFP assay as in (A). Results for 40 J/m^2 could not be reported by the HPRT assay due to high levels of cell death, which lead to no visible colonies formed by the tested HCT116 cells with or without *USP24* KD, in the presence or absence of 6-HT. Further, no statistical significance could be found in control cells treated with 10 J/m^2. Mean cell or colony numbers are shown (±SEM) from three independent experiments.

Statistics: *p < 0.05; **p < 0.01; ****p < 0.0001.

of the CherryOFF-GFP reporter in reporting changes in mutation frequency, we challenged HCT116 cells, with or without *USP24* KD, with increasing dosages of UV irradiation, which is expected to induce many different types of mutation events, including A/T to G/C transitions (Brash, 2015). While *USP24*'s importance regulating mutagenesis following mutagenic stress has been hypothesized (Zhang and Gong, 2016), it has not yet been directly observed. We found that, for the *USP24* KD HCT116 cells, both the HPRT assay and the CherryOFF-GFP assay detected an anticipated increase of mutation at the dose of 10 J/m^2 of UV irradiation compared with the non-stressed condition. This suggests that a reduction of *USP24* indeed increases UV-induced mutation frequency, and that these two assays have similar ability for detecting the change introduced by *USP24* KD. However, the CherryOFF-GFP reporter assay outperformed the HPRT assay in several other situations. This includes the higher UV doses on *USP24* KD HCT116 cells, or for any tested UV dosages with the WT HCT116 cells, which are more vulnerable to UV-induced apoptosis than the *USP24* KD cells (Zhang et al., 2015b). Under these conditions, while the CherryOFF-GFP continued to report an anticipated dose-dependent UV-induced mutation increase, the HPRT assay was either unable to report a statistically significant change or completely failed to generate any meaningful data due to prohibitively high numbers of cell deaths during the incubation time (Figure 3).

These results suggest that the CherryOFF-GFP reporter has the ability to report changes in mutation frequency comparable with the HPRT assay and is capable of displaying mutation frequencies in conditions where the HPRT assay fails. This is largely due to the robustness and speed of the CherryOFF-GFP reporter as designed. Unlike the HPRT assay and many other classic methods that use cell death to distinguish mutant from non-mutant, the CherryOFF-GFP reporter uses the expression of a protein as the readout and therefore is independent of cell death. In addition, the reporter, mCherryFP, is a small protein of ~25 kDa that is transcribed by a potent promoter (cytomegalovirus promoter). Furthermore, the folding and maturation of mCherryFP, like most fluorescence proteins, is robust and independent of chaperones, taking as little as 15 min, and degrades slowly (Shaner et al., 2004). Once the fluorescence signal for mCherryFP is turned on, it should remain detectable as long as

(C) Quantification of the mutation frequencies of HCT116 cells with *USP24* KD or NS control measured with either the HPRT assay (left, blue columns) or the CherryOFF-GFP assay (right, orange columns). See also Figure S3A for representative images for the HPRT assay. The anticipated increase of mutation frequency in *USP24* KD was detected by both assays, although the difference and significance are more obvious in the CherryOFF-GFP assay. Mean cell and colony numbers are shown (±SEM) from three independent experiments. Statistical significance was calculated by Student's t test: *p < 0.05; ***p < 0.001.

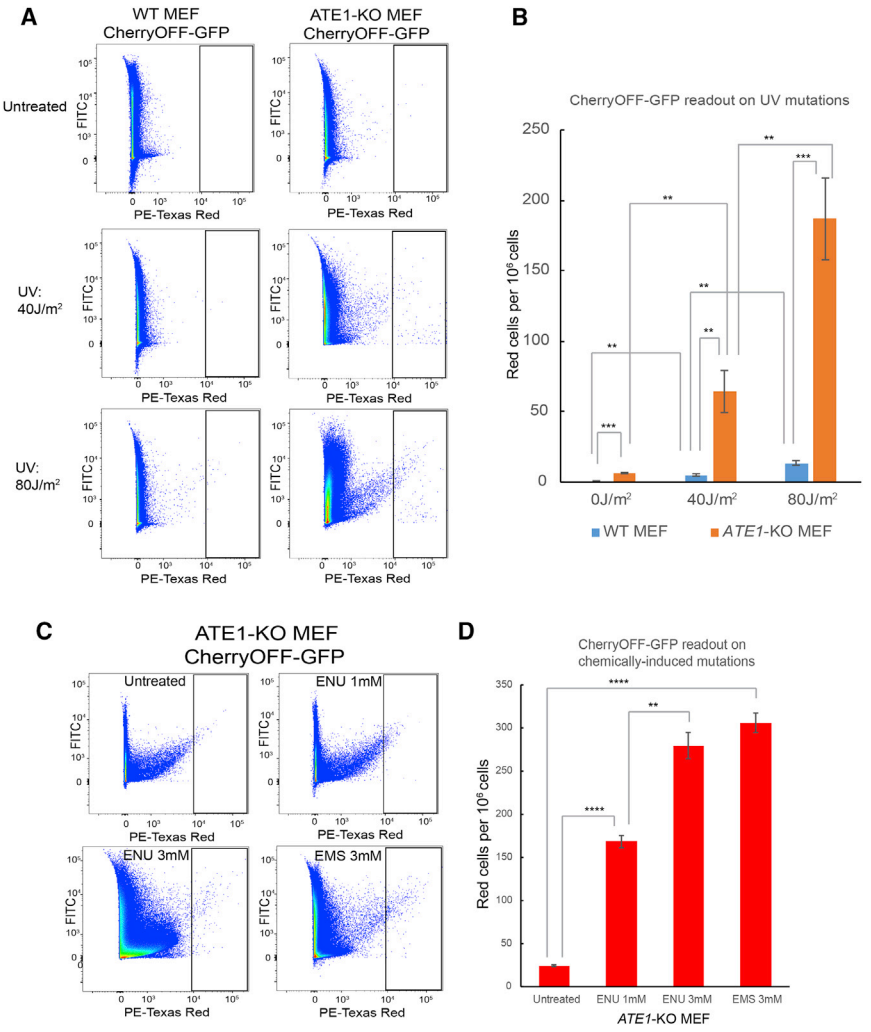

Figure 4. CherryOFF-GFP Accurately Detects Mutagenesis in MEFs with ATE1-KO in a Variety of Conditions

(A) MEFs with or without genomic KO of ATE1 and carrying CherryOFF-GFP were examined for baseline mutagenic activity and mutagenesis following 40–80 J/m^2 UV radiation. Representative flow diagrams show an increase in baseline mutagenesis due to ATE1-KO, and a dose-dependent mutation increase in both cell lines following UV irradiation.

(B) Quantification of (A).

(C) ATE1-KO MEFs were treated with 1 mM or 3 mM N-ethyl-N-nitrosourea (ENU) for 3 days, or 3 mM ethyl methanesulfonate (EMS) for 5 days. Representative flow diagrams show a dose-dependent increase in mutagenesis following ENU treatment and significant mutagenesis following EMS treatment.

(D) Quantification of (C) Mean cell numbers are shown (±SEM) from three independent experiments.

Statistics: **p < 0.01; ***p < 0.001; ****p < 0.0001.

the cell membrane is still intact (Florey et al., 2011). The nature of the readout of this assay, combined with its robustness and speed, allows it to avoid the interference of cell death in readouts.

CherryOFF-GFP Accurately Reports Mutations in a Variety of Cell Types and Conditions

Among traditional mammalian mutation reporters, while the MLA and XPRT assays require specifically engineered cell lines, the HPRT assay is somewhat more flexible and performs in any sufficiently clonogenic cell line. Unfortunately, many cells, including many of those commonly used in research, are non-clonogenic. In addition, as mentioned before, the HPRT assay cannot readily examine the impacts of many factors that also affect cell death/survival or cellular tolerance to cytotoxic reagents. However, in principle, the CherryOFF-GFP reporter should not have any of these limitations.

To demonstrate the capacity of the CherryOFF-GFP reporter in applications with cell lines and conditions unfit for the HPRT assay, we used MEF with or without genomic knockout (KO) of arginyltransferase1 (ATE1). MEF is the most common cell line for studies related to genetic KO. These types of cells, unless highly transformed, rarely grow on soft agar. When grow on culture plate, they are usually highly motile and tend to grow into a monolayer. Therefore, to observe discrete colonies, these cells must be highly diluted during seeding to provide a large area for cells to undergo multiple cell divisions before migrating to nearby colonies. This requirement creates a direct conflict with the needs of seeding a large number of cells for the HPRT assay due to the anticipated cell death following the mutagenic treatments and the treatment of 6-TG. As such, many rounds of trial and error are needed to find an optimal dilution for every single condition. Furthermore, ATE1-KO is known to increase cellular sensitivity to HPRT reagent 6-TG, and is therefore expected to generate false-negative responses for this assay (Zhang et al., 2015a). These above problems make the ATE1-KO MEF highly unsuitable for the HPRT assay but should not adversely affect the CherryOFF-GFP reporter. When we employed CherryOFF-GFP to evaluate mutation frequencies in the WT and ATE1-KO MEF following increasing doses of UV irradiations, we saw a clear dose-dependent increase of red cell ratios in both types of MEFs, with a much higher rate seen in the ATE1-KO cells (Figures 4A and 4B). This was consistent with the known effects of UV irradiation on mutagenesis, as well as with our other studies showing ATE1's role in suppressing mutagenesis (Kumar et al., 2016). Therefore, the CherryOFF-GFP reporter appears to be suitable for cell lines and conditions that are unfit for the HPRT assay, representing a significant advancement for the screening of mutagenic compounds and stressors in custom cellular models of mutagenesis.

To further validate the versatility of CherryOFF-GFP testing for mutagenic factors beyond UV irradiation, we tested this reporter with two chemical mutagens known to cause point

mutations: N-ethyl-N-nitrosourea (ENU) and ethyl methanesulfonate (EMS). ENU mutation has been shown to cause a variety of point mutations in mice, 30%–40% of which are A/T to G/C mutations (Barbaric et al., 2007), which is the mutation required for the CherryOFF-GFP reporter to turn on the mCherryFP expression. EMS causes mutagenesis predominantly by creating G/C to A/T transitions, although an unquantified but small percentage of mutations can be A/T to G/C, at least when tested in bacteriophage T4B (Krieg, 1963). After a 3-day treatment of ENU on ATE1-KO cells carrying CherryOFF-GFP, we found increased amounts of red cells in a dose-dependent manner to ENU concentrations. Also, with exposure to 3 mM EMS with longer duration (5 days), significantly increased red cells were detected in the treated group compared with the untreated (Figures 4C and 4D). These results suggest that this reporter system is capable of measuring effects of any mutagen capable of causing A/T to G/C transitions.

The CherryOFF-GFP Mutation-Activated Reporter Has Low False-Positive Rates

One potential confounding concern for any fluorescence reporter is whether autofluorescence can be erroneously interpreted as a positive signal. To determine the impact of this potential source of error, we repeated representative experiments with or without mutagenic treatments with cell lines only expressing GFP, in which no signal from mCherryFP is expected (Figures S1C and S5A). We found that, in all experimental conditions with the original gate settings, no red signal was passed as a readout in these samples. Considering autofluorescence may also be affected by cell death, we further analyzed GFP-expressing cells treated with the potent apoptosis inducer staurosporine. In conditions where cell death was induced, we did not observe any false-positive reading in our system (Figures S5B and S5C). Therefore, autofluorescence will not affect the readout of our reporter system as long as proper gating is used. Please see STAR Methods for additional suggestions and cautions concerning autofluorescence.

After ruling out the impact of autofluorescence, and based on our findings of mCherryFP's Trp98 dependence, the CherryOFF-GFP reporter potentially has a very low false-positive rate. To examine the specificity of the CherryOFF-GFP reporter assay, we collected UV-irradiated *USP24* KD-HCT116 and *ATE1*-KO MEFs identified as positive mutants (with red fluorescent signal above the gating) in the flow cytometer. When we stabilized these sorted *USP24* KD-HCT116 cells and analyzed their fluorescence under the microscope, we found the vast majority of these cells exhibiting both red and green fluorescence, suggesting that these are true-positive mutant cells. Only a small fraction of less than 1% of cells lacked the red fluorescent signal expected from mCherryFP expression (Figure 5). Furthermore, these erroneous cells may not have been detected by the cytometer as positives but may have originated as cell doublets with mutant and non-mutant cells stuck together in the cytometer, as HCT116 cells are known to adhere to each other in suspension. Indeed, when we examined the sorted ATE1-KO MEFs, which are less adherent (Zhang et al., 2012), the rate of cells that only express the GFP but not the mCherryFP signal is less than 0.12% (Figure 5A).

To further validate the specificity of the CherryOFF-GFP reporter for detecting mutations, we employed a barcode-based next-generation sequencing (NGS) technique, which is known to have the ability to distinguish genetic differences with a resolution of 1 in 1,000 (Pochon et al., 2013; Shao et al., 2016). Indeed, when we tested the resolution of this technique with premixed cell populations, it was able to reach a resolution of 0.1% (Figure 5B). When we used this technique to examine the composition of the ATE1-KO-MEFs that were identified as red positive from flow cytometry, we were only able to detect cells that possess the Trp codon TGG at residue 98. The occurrence of stop codon TGA (or any other codon) at that position is below the anticipated background noise of the NGS detection technique, indicating that the effective false-positive rate must be lower than 0.1% (Figure 5C). It is important to point out that, as mentioned above, the cells without a functional mCherryFP gene may pass the sorter by adhering to the real positive cells. Therefore, these cells may not trigger the red fluorescence detector during fluorescence-activated cell sorting (FACS) analysis and therefore may not present a true false-positive event. However, these cells detected by fluorescence microscopy or NGS analysis represent the upper limit of the true false-positive rate.

The CherryOFF-GFP Mutation-Activated Reporter Can Resolve Time-Dependent Occurrences of Mutation

In mammalian cells, multiple distinct mechanisms with different kinetics exist to govern DNA repair. Also, highly mutated cells are often less fit for long-term survival. As such, the frequency of mutations within a cell population following mutagenic stress can be time dependent (Feng et al., 2016; Wielgoss et al., 2013). However, this fluctuation of mutation burden cannot be monitored by classic mutation reporters due to their requirements for long incubation time. In comparison, the CherryOFF-GFP is a very fast reporting system that has the potential to provide readout with a significantly reduced time delay.

To generate a test model for the changes of mutation burden in a cell population, *ATE1*-KO MEFs carrying the reporter were subjected to the treatment of ENU, which directly alkylate DNA. After the treatment and the removal of ENU, the red fluorescence in the cell population was monitored at different time points. We found that the highest signal for red cells was observable at day 1, the end of the ENU treatment. The ratios of red cells then decreased and eventually reached a steady level at day 3, which is 48 hr after the washout of ENU (Figure 6). To validate that this change of red fluorescence signal is not due to any changes of background or autofluorescence, this experiment was repeated either using cells that do not carry any fluorescent proteins or using those that only express GFP. During the same time points along the ENU treatment, these control cells did not generate any readout for red fluorescence above the threshold (Figure S6). Therefore, the changes of red fluorescence signal in the cells carrying the CherryOFF-GFP must reflect the time-dependent changes of the measurable mutants in the total population. This capacity of the CherryOFF-GFP reporter will accommodate mechanistic studies for the time-dependent changes of mutation burden, which cannot be done with other existing reporter systems.

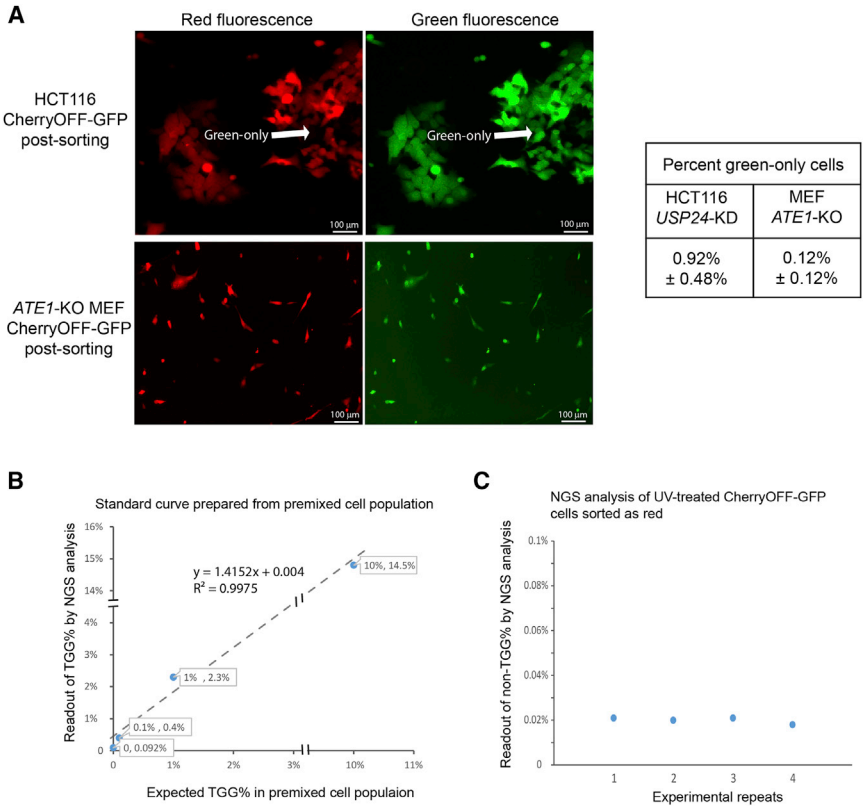

Percent green-only cells	
HCT116 *USP24*-KD	MEF *ATE1*-KO
0.92% ± 0.48%	0.12% ± 0.12%

Figure 5. False-Positive Cells Are Very Rare from CherryOFF-GFP FACS-Detected Red Cells

(A) *USP24* KD HCT116 cells treated with 10 J/m^2 UV, and ATE1-KO MEF cells treated with 40 J/m^2, were sorted and cultured. Representative picture shown with arrow indicating one cell exhibiting only GFP signal in the sorted HCT116 cells. Scale bar represents 100 μm. As shown in the table (right), we found less than 1% green-only cells in HCT cells that were sorted for red fluorescence, which may be due to sticky cell doublets during FACS. In the less self-adhesive MEF cells, a much lower percentage of green-only cells was found in the CherryOFF-GFP carrying cells that were sorted for red signal. Mean cell numbers are shown (±SEM) from three independent experiments.

(B) Standard curve to validate the resolution of next-generation sequencing (NGS) on premixed cell populations. Freshly prepared *ATE1*-KO MEFs containing CherryOFF-GFP or mCherryFP-GFP vectors were isolated and counted. These cells were then mixed in the indicated proportions. Genomic DNA was isolated from the mixed cells (10^7 cells were used for each sample). The region covering residue 98 at the mCherryFP gene was amplified using primers with Illumina adapters. NGS was performed on the resulting amplicons in an Illumina sequencing platform to resolve the occurrences of the stop codon (TGA) and Trp codon (TGG) at the position corresponding to residue 98 of mCherryFP gene. A trend line for linear regression with the corresponding equation and coefficient of determination (R^2) value were computed by the built-in functions of Excel. The results showed that the NGS analysis is able to quantitatively detect the existence of low occurring events at 0.1%. Note that when 0% mCherryFP-GFP-expressing cells were used, a small number of TGG codons were still present in sequencing results, which is most likely due to the spontaneous errors of the technique and naturally occurring reversion in CherryOFF-GFP, which was shown to be 1–2 in 10^5 cells in our analysis (see Figures 4B and 4D).

(C) NGS analysis of red-positive CherryOFF-GFP cells sorted after UV irradiation. Freshly prepared *ATE1*-KO MEFs carrying CherryOFF-GFP were irradiated with 80 J/m^2 UV. After 72 hr, the cells were FACS sorted for red fluorescence and genomic DNA was immediately extracted for NGS analysis. In four independent repeats, the absolute majority of the cells contained Trp codon (TGG) at residue 98 of the mCherryFP gene. A very small number of other types of codons (including TGA) were also present at a frequency of around 0.02%. However, this is likely due to the known spontaneous errors of the NGS technique, particularly considering this percentage represents less than one cell in the input population (repeat 1, 561 cells; repeat 2, 642 cells; repeat 3, 1,057 cells; repeat 4, 583 cells).

DISCUSSION

The CherryOFF-GFP reporter presents many advantages in ease of use, robustness, and speed over previously established mutagenesis assays. As summarized in Figure 7, once the desired cell line is established with the CherryOFF-GFP gene incorporated, testing for mutagenesis is fast, cheap, and does not require any special media or chemicals. In addition, the CherryOFF-GFP reporter is independent of cell survival/death and therefore can specifically evaluate the impacts of many factors on mutation separately from cell survival/death. Furthermore, the CherryOFF-GFP reporter has no cell line limitation and can be easily adapted to almost any cell or system that actively expresses proteins. As such, this tool will become useful for studying evolution, cancer, and any other mutation-related topics. This reporter can be efficiently applied to many industrial settings. For example, the environment protection, forensic, and anti-terrorism agencies can use the CherryOFF-GFP as a more rapid alternative to the currently used HPRT assay for evaluating genotoxicity of chemical or physical factors. Also, this reporter can be used to measure mutagenic effects of radiation and chemotherapeutic chemicals at highly lethal dosages, which are important data for balancing the benefits and risks of medical treatments but cannot be obtained with classic methods. For academic research, this reporter can be easily adapted to measure the mutagenic impacts of genetic or epigenetic factors without worrying about complications such as cell death. Furthermore, in principle, the CherryOFF-GFP can cross-compare cells from different genetic backgrounds, allowing evaluation of the mutation frequencies between different tissues of the same animal, different individuals of the same species, or even different species. This reporter may even be used with *in vivo* models to study the mutagenic effects in xenograft tissues or transgenic models. These capacities of the CherryOFF-GFP reporter will accommodate mechanistic studies that cannot be done with other existing reporter systems.

Another significant advantage of this reporter is its speed, which allows it to report time-dependent changes of mutation burden in a population. This capacity may facilitate mechanistic studies for the variation of genomic stability. Such

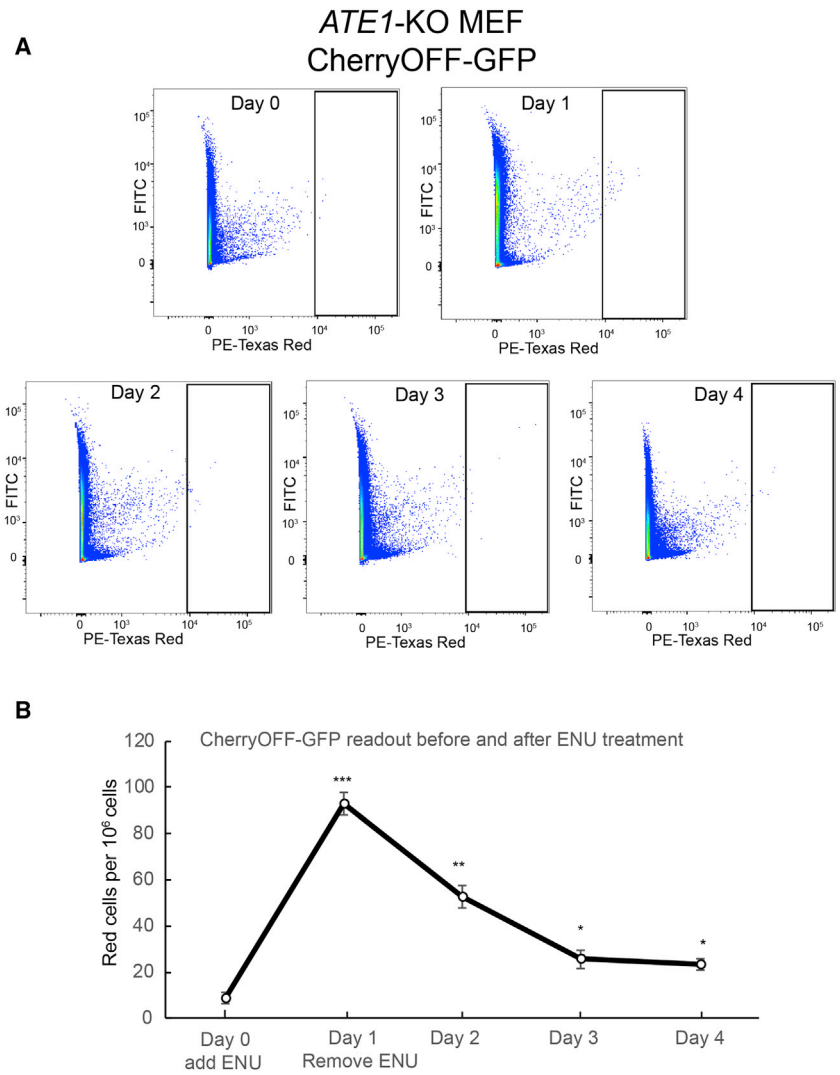

Figure 6. Time Course of CherryOFF-GFP Signal Following Mutagenic Chemical Treatment in ATE1-KO MEF

(A) Representative flow diagrams of ATE1-KO MEFs transduced with CherryOFF-GFP starting at day 0 before treatment. The cells with CherryOFF-GFP were then treated for 24 hr with 1 mM ENU, followed by washing to remove the chemical. The cells were analyzed on day 1 to day 4 and representative flow charts are displayed respectively. CherryOFF-GFP signal peaked at day 1, and gradually reduced until reaching a stable point at day 3 and day 4.

(B) Quantification of (A). See also Figure S6 for the lack of mutation signals in ENU-treated cells that do not carry the full version of the reporter. Mean cell numbers are shown (±SEM) from three independent experiments. Statistics: *p < 0.05; **p < 0.01; ***p < 0.001.

variations have been anticipated during physiological processes such as DNA damage/repair, cell development/differentiation, or the acquisition of stemness, but have not been sufficiently studied due to the limitation of tools. This reporter can also be adapted to quantify mutations occurring *de novo* after the first round of measurement, simply by preserving the cells not expressing red fluorescence at the first round of analysis for the next measurement. By a similar principle, this assay would allow the measurement of new mutations per cell division by sorting out red cells at each cell division to allow the observation of emergent new mutants on a continuous time basis. In addition, the speed of the CherryOFF-GFP reporter and its needlessness for a plating efficiency control would help to avoid many operational errors that may inadvertently affect the results in classic methods that rely on cell death for readouts.

Our data demonstrated that the mutation-activated reporter CherryOFF-GFP generates very few experimental false-positives. The most probable source of error for this assay would be associated with the stringency of gating criteria during analysis of flow cytometry data. However, as long as the gating is set up using appropriate positive and negative control cells, background and noise fluorescence from events such as apoptosis or an erroneous readthrough of the premature termination codon should not generate sufficient whole-cell fluorescence for detection (Figure S1) (Hofhuis et al., 2016). Another potential source of false signal may derive from erroneous transcription on lesioned genomic materials. The impact of such a scenario is expected to be limited due to the low kinetics of these types of processes (Walmacq et al., 2015; Wang et al., 2018). Additional barriers against such false signals include the requirement of Trp98 for the fluorescence of mCherryFP and the high threshold setup for the detection of positive events. However, as a precaution, key conclusions from the reporter assay should be validated by alternative methods, which include NGS analysis on the identified red-positive cells.

The nature of this reporter assay is designed to reflect relative changes by comparing with appropriate controls. Therefore, even though the change in gating would affect the absolute signal value of individual samples, the relative values normalized to the control group should remain less affected. As an additional note, due to spontaneous mutation, the stabilized cell lines carrying CherryOFF-GFP may accumulate red cells in a population, leading to an increase of baseline red cells in late passages of the test cell line. If necessary, these mutated cells can be sorted out during the optional preclearing step, as shown in Figure 7.

Our assay utilizes the Trp98 dependence of mCherryFP and specifically measures A to G (or T to C) transitions, which are nucleotide transition events between two purines or two pyrimidines and are expected to be commonly present in most naturally occurring mutagenic conditions. Due to the high accuracy and low false-positive rate of this assay, it is effective at providing positive responses to a wide variety of DNA-damaging stressors, even when only a small fraction of the expected mutations are nucleotide transitions. While the mutation spectra

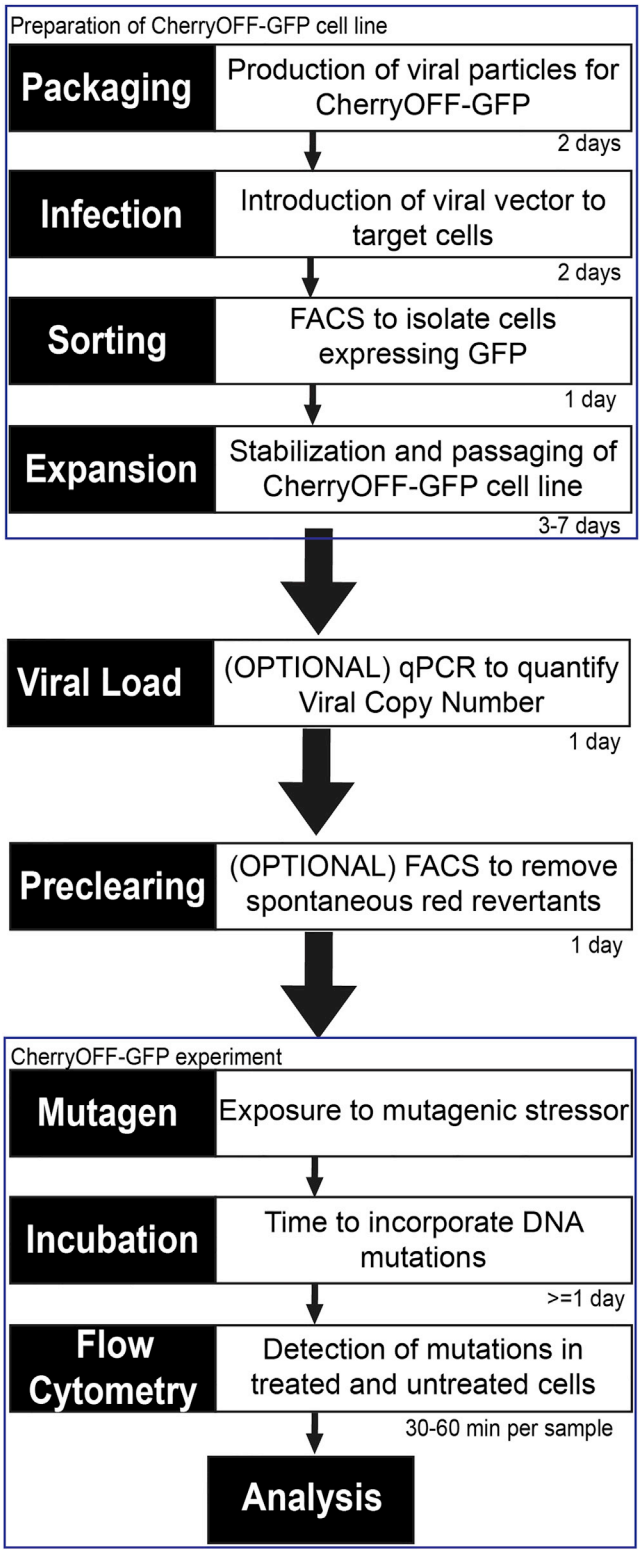

Figure 7. Diagram Representing Workflow and Estimated Times to Establish a CherryOFF-GFP Cell Line and Perform CherryOFF-GFP Experiments

Establishing a cell line for permanent use can be accomplished in as little as 1 week. Stabilized CherryOFF-GFP cell lines can then be deployed in experiments in as little as 1 day, giving a short turnaround time for this assay.

detected by this reporter detects are very narrow, the reporter remains adequate to detect small changes in mutation frequency thanks to its low background noise. Although in principle the CherryOFF-GFP reporter requires more cells than the HPRT assay to generate statistically significant data, the required cell number is typically in the range of 3 to 10 million and should not be a limitation for most real-life applications. Further, the narrow spectra may be an advantage, because different mutation events can be distinguished by different versions of the CherryOFF-GFP reporter. For example, UV more commonly generates C-to-T transitions. The CherryOFF-GFP reporter could experience greatly increased sensitivity to UV by employing a CGA (arginine) at the 98th residue, to specifically detect a C-to-T mutation event. Additional reporters can be generated based on a similar principle on the other fluorescence-essential residues, such as the tri-peptide chromophore, to make possible the detection of other types of mutations, including alternate point mutations, and small insertions and deletions.

SIGNIFICANCE

In this study, we described a mutagenesis reporter that is fast, versatile, robust, and independent of cell lines. It will become a powerful tool for people who study cancer-related or DNA-damage-related mechanisms, evaluate genotoxic effects of physical factors and or chemicals, and investigate molecular evolution, in academic and industry settings.

STAR★METHODS

Detailed methods are provided in the online version of this paper and include the following:

- KEY RESOURCES TABLE
- CONTACT FOR REAGENT AND RESOURCE SHARING
- EXPERIMENTAL MODEL AND SUBJECT DETAILS
  - Mammalian Cells and Media
- METHOD DETAILS
  - Preparation of Cell Lines Carrying the CherryOFF-GFP Reporter
  - Knockdown of USP24
  - Genomic DNA Purification
  - Quantitative PCR
  - Examining Viral Copy Number (VCN)
  - UV Irradiation
  - Chemical Mutagenesis
  - Staurosporine Treatment
  - Flow Cytometry Analysis and Fluorescence-Activated Cell Sorting (FACS)
  - HPRT Mutagenesis Assay
  - Molecular Cloning and Construction of Plasmids
  - Next-Generation-Sequencing (NGS) of Genomic DNA Region Containing CherryOFF or mCherryFP
  - Molmil Structural Analysis
  - Microscopy
  - Cell Counting
  - Analysis of Flow Cytometry Data
- QUANTIFICATION AND STATISTICAL ANALYSIS
- DATA AND SOFTWARE AVAILABILITY

SUPPLEMENTAL INFORMATION

Supplemental Information includes six figures and one table and can be found with this article online at https://doi.org/10.1016/j.chembiol.2018.05.010.

ACKNOWLEDGMENTS

We thank the flow cytometry core facility at the Sylvester Comprehensive Cancer Center, and the Sequencing Center for Genome Technology (CGT) at the John P. Hussman Institute for Human Genomics of the University of Miami for providing services for experiments related to this study. We also thank Dr. Hua Chen, from the laboratory of Dr. Murray Deutscher in the Department of Biochemistry and Molecular Biology at the University of Miami, who provided technical assistance with the Bio-Rad MJ Mini thermal cycler. We also thank Dr. Vladlen Slepak and Dr. Daniel Isom in the Department of Molecular and Cellular Pharmacology at the University of Miami for providing critical reading of this manuscript. This study is supported by these funding resources: NIGMS/NIH, R01#GM107333; DOD (CDMRP), Idea Award, PC140622.

AUTHOR CONTRIBUTIONS

M.D.B. participated in the design of the original CherryOFF-GFP reporter vector, designed and performed the majority of the experiments, and analyzed corresponding data as present in all the figures. L.N. performed the small hairpin RNA knockdown of *USP24*, and also performed the HPRT assays. A.K. participated in the design of the original CherryOFF-GFP reporter vector. F.Z. and F.G. designed the strategy of the project, and supervised the performance of related experiments and the analysis of data.

DECLARATION OF INTERESTS

The mutation-activated fluorescence reporter is covered by a pending international patent (WO, 2018/064571) with F.Z., M.B., and A.K. as inventors.

The authors declare no other conflict of interest.

Received: June 20, 2017
Revised: February 26, 2018
Accepted: May 11, 2018
Published: June 14, 2018

REFERENCES

Barbaric, I., Wells, S., Russ, A., and Dear, T.N. (2007). Spectrum of ENU-induced mutations in phenotype-driven and gene-driven screens in the mouse. Environ. Mol. Mutagen. *48*, 124–142.

Bekker, G.-J., Nakamura, H., and Kinjo, A.R. (2016). Molmil: a molecular viewer for the PDB and beyond. J. Cheminform. *8*, 42.

Brash, D.E. (2015). UV signature mutations. Photochem. Photobiol. *91*, 15–26.

Dean, L. (2012). Thioguanine therapy and TPMT genotype. In Medical Genetics Summaries, V. Pratt, H. McLeod, L. Dean, A. Malheiro, and W. Rubinstein, eds. (National Center for Biotechnology Information (US)).

Feng, Y., Jonker, M.J., Moustakas, I., Brul, S., and Ter Kuile, B.H. (2016). Dynamics of mutations during development of resistance by Pseudomonas aeruginosa against five antibiotics. Antimicrob. Agents Chemother. *60*, 4229–4236.

Florey, O., Kim, S.E., Sandoval, C.P., Haynes, C.M., and Overholtzer, M. (2011). Autophagy machinery mediates macroendocytic processing and entotic cell death by targeting single membranes. Nat. Cell Biol. *13*, 1335–1343.

Fu, J.L., Kanno, T., Liang, S.C., Matzke, A.J., and Matzke, M. (2015). GFP loss-of-function mutations in Arabidopsis thaliana. G3 (Bethesda) *5*, 1849–1855.

Gad, S.C., ed. (2008). Preclinical development handbook. Toxicology (Wiley-Interscience).

Gefen, N., Brkic, G., Galron, D., Priel, E., Ozer, J., Benharroch, D., and Gopas, J. (2010). Acquired resistance to 6-thioguanine in melanoma cells involves the repair enzyme O6-methylguanine-DNA methyltransferase (MGMT). Cancer Biol. Ther. *9*, 49–55.

Giono, L.E., and Manfredi, J.J. (2006). The p53 tumor suppressor participates in multiple cell cycle checkpoints. J. Cell. Physiol. *209*, 13–20.

Hofhuis, J., Schueren, F., Notzel, C., Lingner, T., Gartner, J., Jahn, O., and Thoms, S. (2016). The functional readthrough extension of malate dehydrogenase reveals a modification of the genetic code. Open Biol. *6*, https://doi.org/10.1098/rsob.160246.

Ichikawa, M., Nakane, H., Marra, G., Corti, C., Jiricny, J., Fitch, M., Ford, J.M., Ikejima, M., Shimada, T., Yoshino, M., et al. (2000). Decreased UV sensitivity, mismatch repair activity and abnormal cell cycle checkpoints in skin cancer cell lines derived from UVB-irradiated XPA-deficient mice. Mutat. Res. *459*, 285–298.

Johnson, G.E. (2012). Mammalian cell HPRT gene mutation assay: test methods. Methods Mol. Biol. *817*, 55–67.

Krieg, D.R. (1963). Ethyl methanesulfonate-induced reversion of bacteriophage T4rII mutants. Genetics *48*, 561–580.

Kumar, A., Birnbaum, M.D., Patel, D.M., Morgan, W.M., Singh, J., Barrientos, A., and Zhang, F. (2016). Posttranslational arginylation enzyme Ate1 affects DNA mutagenesis by regulating stress response. Cell Death Dis. *7*, e2378.

Kwon, Y.T., Kashina, A.S., Davydov, I.V., Hu, R.G., An, J.Y., Seo, J.W., Du, F., and Varshavsky, A. (2002). An essential role of N-terminal arginylation in cardiovascular development. Science *297*, 96–99.

Ma, Y., Zhang, J., Yin, W., Zhang, Z., Song, Y., and Chang, X. (2016). Targeted AID-mediated mutagenesis (TAM) enables efficient genomic diversification in mammalian cells. Nat. Methods *13*, 1029–1035.

Mortelmans, K., and Zeiger, E. (2000). The Ames *Salmonella*/microsome mutagenicity assay. Mutat. Res. *455*, 29–60.

Newman, A.M., Bratman, S.V., To, J., Wynne, J.F., Eclov, N.C., Modlin, L.A., Liu, C.L., Neal, J.W., Wakelee, H.A., Merritt, R.E., et al. (2014). An ultrasensitive method for quantitating circulating tumor DNA with broad patient coverage. Nat. Med. *20*, 548–554.

Pochon, X., Bott, N.J., Smith, K.F., and Wood, S.A. (2013). Evaluating detection limits of next-generation sequencing for the surveillance and monitoring of international marine pests. PLoS One *8*, e73935.

Ro, S. (2004). Magnifying stem cell lineages: the stop-EGFP mouse. Cell Cycle *3*, 1246–1249.

Shaner, N.C., Campbell, R.E., Steinbach, P.A., Giepmans, B.N., Palmer, A.E., and Tsien, R.Y. (2004). Improved monomeric red, orange and yellow fluorescent proteins derived from *Discosoma* sp. red fluorescent protein. Nat. Biotechnol. *22*, 1567–1572.

Shao, D., Lin, Y., Liu, J., Wan, L., Liu, Z., Cheng, S., Fei, L., Deng, R., Wang, J., Chen, X., et al. (2016). A targeted next-generation sequencing method for identifying clinically relevant mutation profiles in lung adenocarcinoma. Sci. Rep. *6*, 22338.

Shor, E., Fox, C.A., and Broach, J.R. (2013). The yeast environmental stress response regulates mutagenesis induced by proteotoxic stress. PLoS Genet. *9*, e1003680.

Shu, X., Shaner, N.C., Yarbrough, C.A., Tsien, R.Y., and Remington, S.J. (2006). Novel chromophores and buried charges control color in mFruits. Biochemistry *45*, 9639–9647.

Song, M.S., Salmena, L., and Pandolfi, P.P. (2012). The functions and regulation of the PTEN tumour suppressor. Nat. Rev. Mol. Cell Biol. *13*, 283–296.

Stewart, S.A., Dykxhoorn, D.M., Palliser, D., Mizuno, H., Yu, E.Y., An, D.S., Sabatini, D.M., Chen, I.S., Hahn, W.C., Sharp, P.A., et al. (2003). Lentivirus-delivered stable gene silencing by RNAi in primary cells. RNA *9*, 493–501.

Tichy, E.D., Liang, L., Deng, L., Tischfield, J., Schwemberger, S., Babcock, G., and Stambrook, P.J. (2011). Mismatch and base excision repair proficiency in murine embryonic stem cells. DNA Repair (Amst) *10*, 445–451.

Vogelstein, B., Lane, D., and Levine, A.J. (2000). Surfing the p53 network. Nature *408*, 307–310.

Walmacq, C., Wang, L., Chong, J., Scibelli, K., Lubkowska, L., Gnatt, A., Brooks, P.J., Wang, D., and Kashlev, M. (2015). Mechanism of RNA polymerase II bypass of oxidative cyclopurine DNA lesions. Proc. Natl. Acad. Sci. USA *112*, E410–E419.

Wang, W., Walmacq, C., Chong, J., Kashlev, M., and Wang, D. (2018). Structural basis of transcriptional stalling and bypass of abasic DNA lesion by RNA polymerase II. Proc. Natl. Acad. Sci. USA *115*, E2538–E2545.

Wielgoss, S., Barrick, J.E., Tenaillon, O., Wiser, M.J., Dittmar, W.J., Cruveiller, S., Chane-Woon-Ming, B., Medigue, C., Lenski, R.E., and Schneider, D. (2013). Mutation rate dynamics in a bacterial population reflect tension between adaptation and genetic load. Proc. Natl. Acad. Sci. USA *110*, 222–227.

Zhang, F., Saha, S., and Kashina, A. (2012). Arginylation-dependent regulation of a proteolytic product of talin is essential for cell-cell adhesion. J. Cell Biol. *197*, 819–836.

Zhang, F., Patel, D.M., Colavita, K., Rodionova, I., Buckley, B., Scott, D.A., Kumar, A., Shabalina, S.A., Saha, S., Chernov, M., et al. (2015a). Arginylation regulates purine nucleotide biosynthesis by enhancing the activity of phosphoribosyl pyrophosphate synthase. Nat. Commun. *6*, 7517.

Zhang, L., Nemzow, L., Chen, H., Lubin, A., Rong, X., Sun, Z., Harris, T.K., and Gong, F. (2015b). The deubiquitinating enzyme USP24 is a regulator of the UV damage response. Cell Rep. *10*, 140–147.

Zhang, L., and Gong, F. (2016). Involvement of USP24 in the DNA damage response. Mol. Cell. Oncol. *3*, e1011888.

STAR★METHODS

KEY RESOURCES TABLE

REAGENT or RESOURCE	SOURCE	IDENTIFIER
Antibodies		
Rabbit anti-USP24	Origene	Cat#TA315240; RRID: AB_2722752
Mouse anti-tubulin	Santa Cruz	Cat#H-235; RRID: AB_2241191
Bacterial and Virus Strains		
Lentiviral particles encoding USP24 shRNA	Sigma	Cat#SHCLNV-NM_015306
Lentiviral particles encoding scrambled shRNA	Sigma	Cat#SHC002V
TOP10 Chemically Competent E. coli	Thermo Fischer	Cat#C404010
Chemicals, Peptides, and Recombinant Proteins		
Puromycin	ThermoFisher	Cat#A1113802; CAS: 58-58-2
6-thioguanine	Sigma	Cat#A4882; CAS: 154-42-7
Polyethyleneimine	Sigma	Cat#408727; CAS: 9002-98-6
N-ethyl-N-nitrosourea	Sigma	Cat#N3385; CAS: 759-73-9
Ethyl methanesulfonate	Sigma	Cat#M0880; CAS: 62-50-0
Staurosporine	Enzo Life Sciences	Cat#ALX-380-014-C100; CAS: 62996-74-1
Proteinase K	New England Biolabs	Cat#P8107; CAS: 39450-01-6
Critical Commercial Assays		
gDNA isolation kit	Amresco	Cat#VWRVK368
SSOAdvanced Universal SYBR Green Supermix	Bio-Rad	Cat#1725270
Experimental Models: Cell Lines		
MEF	Kwon et al., 2002	https://www.ncbi.nlm.nih.gov/pubmed/12098698
MEF Ate1-KO	Kwon et al., 2002	https://www.ncbi.nlm.nih.gov/pubmed/12098698
HCT116	ATCC	ATCC CCL-247
HEK293T	ATCC	ATCC CRL-11268
Oligonucleotides		
See Table S1		N/A
Recombinant DNA		
Delta R8.2	N/A	Addgene 12263
VSV-G	Stewart et al., 2003	Addgene 8454
pQC-XIG	N/A	Addgene 26826
Software and Algorithms		
FlowJo v10	FlowJo, LLC	https://www.flowjo.com/
FacsDIVA 6.1.3	BD	http://www.bdbiosciences.com/ca/instruments/clinical/software/flow-cytometry-acquisition/bd-facsdiva-software/bd-facsdiva-software-v-613/p/643629
gVIM v7.3	VimOnline	https://www.vim.org
HiSeq 3000	Illumina	https://www.illumina.com/systems/sequencing-platforms/hiseq-3000-4000.html
MiSeq v2.5	Illumina	https://www.illumina.com/systems/sequencing-platforms/miseq.html
CFX 3.1 manager	BioRad	http://www.bio-rad.com/en-us/sku/1845000-cfx-manager-software?ID=1845000
Deposited Data		
pQC-mCherryFP-GFP	This Paper	https://doi.org/10.17632/d56h7fdtjw.1
pQC-CherryOFF-GFP	This Paper	https://doi.org/10.17632/d56h7fdtjw.1

(*Continued on next page*)

Continued

REAGENT or RESOURCE	SOURCE	IDENTIFIER
NGS reads of the CherryOFF region in the genomic DNA extracts after UV treatments	This Paper	https://doi.org/10.17632/d56h7fdtjw.1
NGS reads of premixed mCherryFP-GFP and CherryOFF-GFP genomic DNA extracts (standard curve)	This Paper	https://doi.org/10.17632/d56h7fdtjw.1

CONTACT FOR REAGENT AND RESOURCE SHARING

Further information and requests for resources and reagents should be directed to and will be fulfilled by the Lead Contact. Dr. Fangliang Zhang (fzhang2@miami.edu).

EXPERIMENTAL MODEL AND SUBJECT DETAILS

Mammalian Cells and Media

Immortalized mouse embryonic fibroblasts (MEFs) carrying either wild-type ATE1 or knockout of ATE1 (ATE1-KO) were a gift from Dr. Anna Kashina (University of Pennsylvania), and were originally isolated from mouse embryos carrying complete genomic Ate1-KO or a wild-type genome (Kwon et al., 2002). Both MEF cell lines were derived from female embryos. Human embryonic kidney cell line (HEK 293T; clone T7, female origin) and human colorectal carcinoma cell line (HCT116; clone CCL247, male origin) were obtained from ATCC (Manassas, VA).

Mammalian cells were grown in DMEM high glucose (Life Technologies, Cat# 11995-065) supplemented with 10% FBS (HyClone, Cat# SH30910.03), maintained at 37°C under 5% CO2. Cells were detached using 0.25% Trypsin solution (Life Technologies, Cat# 25200-072).

METHOD DETAILS

Preparation of Cell Lines Carrying the CherryOFF-GFP Reporter

Lentiviral particles for CherryOFF-GFP were packaged in HEK 293T cells using helper plasmids Delta R8.2 and VSV-G. Delta R8.2 was a gift from Didier Trono (Addgene plasmid #12263), and VSV-G was a gift from Bob Weinberg (Addgene plasmid #8454)), transfected with Polyethyleneimine (PEI) (Sigma Aldrich). Viral particles were harvested 24 hours after initial transfection, filtered through a 0.45-uM syringe filter, supplemented with 10ug/mL polybrene, then immediately added to their target cells. To minimize the possibility of multiple viral insertions per cell, the amount of virus was titrated. The concentration of virus used resulted in less than 10% of cells being infected (judging by the green fluorescence) while the maximal infected rates with saturated amount of virus are ~30%. Three days following infection, cells were sorted for GFP alongside untransduced control cells to set cutoff threshold to exclude all non-fluorescent cells.

To minimize the accumulation of red revertant cells originating from spontaneous mutation in the populations, early passages of the sorted cells were used in most experiments conducted in this study unless otherwise indicated.

Knockdown of USP24

HCT116 cells stably transduced with the CherryOFF-GFP reporter were employed for further USP24-knockdown or a mock knockdown control. Lentiviral particles were purchased from Sigma Aldrich encoding shRNA sequences against human USP24 and non-silencing control (SHCLNV-NM_015306 and SHC002V). 5uL of lentiviral particles were used to infect a 60mm dish of HCT116 cells, and then selected with 5ug/mL puromycin. USP24 knockdown efficiency was quantified via western blot using a rabbit-anti-USP24 antibody (Origene TA5240) compared to tubulin control (Santa Cruz H-235)

Genomic DNA Purification

Genomic DNA was extracted from cells with Cyclo-Prep Genomic DNA isolation kit (Amresco) and proteinase K (New England Biolabs).

Quantitative PCR

qPCR was performed on gDNA using a Bio-Rad MJ Mini thermal cycler equipped with a MiniOpticon RT-PCR detection system, using Bio-Rad SSOAdvanced SYBR Green Supermix. Analysis of the PCR results was performed with Bio-Rad CFX Manager 3.1.

Examining Viral Copy Number (VCN)

Genomic DNA were extracted from virus-transduced cells carrying the CherryOFF-reporter. Quantitative PCR was then used to measure the level of the viral insert in the genomic DNA, by comparing the level of GFP gene to β-actin (as loading control).

The following primers specific for GFP were used to measure the level of the CherryOFF-GFP reporter:
GFP-forward: 5′-ACGTAAACGGCCACAAGTTC-3′
GFP-reverse: 5′-AAGTCGTGCTGCTTCATGTG-3′
These following primers specific for mouse and human β-actin were used as loading control for the genomic DNA:
Actin forward: 5′-AAATCTGGCACCACACCTTC-3′
Actin reverse: 5′-GGGGTGTTGAAGGTCTCAAA-3′
Our analysis showed that the two cell pairs (WT MEF v.s. ATE1-KO MEF; USP24-knockdown HCT116 v.s. nonsilencing HCT116) have similar level of viral inserts in their genome (Figure S1A).

UV Irradiation

Mammalian cells (HCT116 or MEFs) were plated 24 hours before irradiation. Immediately prior to irradiation, media was aspirated and the cells were briefly washed with dPBS. With lids and dPBS removed, culture plates containing the cells were exposed directly to UV-C radiation in a 254nm UV oven (CL-1000S UV crosslinker, UVP), then media was replenished. All experiments here involved two equal doses of UV radiation, 24 hours apart. Reported radiation doses are the total combined dose from two treatments. Unless otherwise indicated, 48 hours following the terminal dose, cells were trypsinized and resuspended in serum-free media for flow cytometry analysis or sorting.

Chemical Mutagenesis

Chemical mutagenesis assays were done by supplementing ATE1-KO MEFs carrying CherryOFF-GFP with 1mM or 3mM ENU (Sigma-Aldrich, N3385) for 3 days, and 3mM EMS (Sigma-Aldrich, M0880) for 5 days. Media and drug were changed at 48 hour time points until analysis on day 5 past the initiation of treatment.

For measuring the time-dependent changes of mutation frequencies, the cells were incubated with 1mM ENU for 24 hours. The medium containing the chemical was then removed, and the cells were washed with dPBS before supplemented with normal cell culture medium for the rest duration. The cells were analyzed with FACS at an interval of 24 hours through the time course.

Staurosporine Treatment

Ate1-KO MEF cells either stably transduced with pQC-XIG, or not transduced, were treated with the indicated doses of Staurosporine (STS) (from Enzo Life Sciences, Cat#ALX-380-014-C100) for 24 hours. At the end of 24 hours, all the cells in the suspension were collected. The remaining attached cells were also collected by trypsinization and pull together with the suspended cells. A portion of these cells was trypan-blue stained for counting and assessment of cell death, and the remaining were analyzed for green and red fluorescence via FACS.

Flow Cytometry Analysis and Fluorescence-Activated Cell Sorting (FACS)

Flow cytometry analysis or sorting was performed on a BD Aria-IIu flow cytometer in the core facility of the Sylvester Comprehensive Cancer Center at the University of Miami. To minimize background fluorescence, cell fragments or aggregates were excluded based on size using side scatter and forward scatter. The remaining cells were measured for fluorescence in PE-Texas red and FITC channels, which will detect the fluorescence signals of the mCherryFP and GFP, respectively.

HPRT Mutagenesis Assay

For each testing condition, 200,000 cells were plated onto a 60mm dish and treated with 5ug/mL 6-TG. Media with fresh 6-TG was changed every 3 days for 10-14 days until visible colonies appear. The cells were then fixed with 4% PFA in PBS for 30 minutes, then stained with Crystal Violet. Colonies greater than 50 cells were counted. This assay did not utilize HAT treatment for pre-clearing, because our USP24 model was not known to suffer from prohibitively high background.

To calculate plating efficiency, 200 cells were plated onto a 60mm dish in complete media, and allowed to grow for several days until colonies formed. After fixing and staining, colonies were counted, and a ratio of viable colonies to plated cells was used to compensate for nonviable cells.

Molecular Cloning and Construction of Plasmids

All molecular cloning work was performed with high-fidelity DNA polymerase Herculase (Agilent Technologies). Ligation products were transformed into chemical competent E. coli TOP10 (Life Technologies).

PCR reactions were performed in either a Veriti Thermo Cycler (Applied Biosystems) or a T100 Thermo Cycler (BioRad). Primers were ordered from IDT or Sigma.

The coding sequence of mCherryFP was amplified from a template plasmid as described previously (Zhang et al., 2012)by these following primers:
Xho1-mCherryFP-Forward: 5′-TTAACTCGAGATTGATCCGCATGGTG-3′
Not1-mCherryFP-Reverse: 5′-TTAAGCGGCCGCCGGAATTTTACTTGTAC-3′
The corresponding PCR product was then inserted into the plasmid pQC-XIG (w497-1), which was a gift from Eric Campeau (Addgene plasmid #26826), resulting in the coding sequences of mCherryFP and eGFP being driven by the same CMV promoter and separated by an internal ribosome entry site (IRES).

On the basis of this vector, the CherryOFF reporter and the mutated mCherryFP with different amino acids at residues 98 were constructed by overlapping-primer PCR mutation with the following primers:

CherryOFF-Forward: 5′-ccccgagggcttcaagtgAgagcgcgtgatgaacttcg-3′
CherryOFF-Reverse: 5′-cgaagttcatcacgcgctcTcacttgaagccctcgggg-3′
Cys98-Forward: 5′-ccccgagggcttcaagtgTgagcgcgtgatgaacttcg-3′
Cys98-Reverse: 5′-cgaagttcatcacgcgctcAcacttgaagccctcgggg-3′
Gly98-Forward: 5′-ccccgagggcttcaagGgAgagcgcgtgatgaacttcg-3′
Gly98-Reverse: 5′-cgaagttcatcacgcgctcTcCcttgaagccctcgggg-3′
Ser98-Forward: 5′-ccccgagggcttcaagtCAgagcgcgtgatgaacttcg-3′
Ser98-Reverse: 5′-cgaagttcatcacgcgctcTGacttgaagccctcgggg-3′
Arg98-Forward: 5′-ccccgagggcttcaagCgAgagcgcgtgatgaacttcg-3′
Arg98-Reverse: 5′-cgaagttcatcacgcgctcTcGcttgaagccctcgggg-3′
Leu98-Forward: 5′-ccccgagggcttcaagtTAgagcgcgtgatgaacttcg-3′
Leu98-Reverse: 5′-cgaagttcatcacgcgctcTAacttgaagccctcgggg-3′

Next-Generation-Sequencing (NGS) of Genomic DNA Region Containing CherryOFF or mCherryFP

For the preparation of standard curves, freshly prepared ATE1-KO MEF carrying CherryOFF-GFP or mCherryFP-GFP were collected by sorting for green fluorescence and then mixed with indicated ratios. For the measurement of false positive in mutant cells identified as red, 10 million Ate1-KO MEF carrying CherryOFF-GFP were treated with 80J/m^2 UV irradiation, and then sorted 72 hours later by flow cytometry to isolate cells that pass the threshold for red signal as described in other section. A two-step PCR strategy was used for NGS analysis of genomic DNA extracted from these cells. First round primers were specific for mCherryFP/CherryOFF coding region and containing random barcode and Illumina adapters . In the first-round PCR, a reaction of 2 cycles was performed for samples prepared from large numbers of cells, and 10 cycles was performed for low-input (<1000) cell samples as previous studies have demonstrated (Newman et al., 2014). The resulting products were then subjected to second-round amplification using standard Illumina index primers with standard protocol (Newman et al., 2014). All PCR was performed with high-fidelity polymerase Herculase (Agilent). NGS data was generated utilizing the Illumina HiSeq 3000 and MiSeq v2.5 platforms. The primers used in NGS are listed as below:

First round NSG forward primer:
5′-CACGACGCTCTTCCGATCTNNNNNNNNTTGAAGCTGTCCTTCCCCGA-3′
First round NGS reverse primer
5′-CAGACGTGTGCTCTTCCGATCTGTCCTCGAAGTTCATCACGCGC-3′Second round NGS Illumina forward primer:
5′-AATGATACGGCGACCACCGAGATCTACACTCTTTCCCTACACGACGCTCTTCCGATCT-3′
Second round NGS reverse primer
index 1 :
5′-CAAGCAGAAGACGGCATACGAGATGTCGGTAAGTGACTGGAGTTCAGACGTGTGCTCTTCCGATCT-3′
index 2 :
5′-CAAGCAGAAGACGGCATACGAGATAGGTCACTGTGACTGGAGTTCAGACGTGTGCTCTTCCGATCT-3′
index 3 :
5′-CAAGCAGAAGACGGCATACGAGATGAATCCGAGTGACTGGAGTTCAGACGTGTGCTCTTCCGATCT-3′
index 4 :
5′-CAAGCAGAAGACGGCATACGAGATGTACCTTGGTGACTGGAGTTCAGACGTGTGCTCTTCCGATCT-3′

MolMil Structural Analysis

mCherryFP's structure (PDB ID 2H5Q) as analyzed and deposited by Shu et al (Shu et al., 2006) was visualized using PDBj.org's built-in MolMil structure visualization tool (Bekker et al., 2016). mCherryFP's structure was accessed via PDBj.org, and the structure was viewed using a ribbon structural view. Trp98 was accented and visualized at the chromophore by using ball-and-stick visualization at that select residue.

Microscopy

Optical and fluorescent imaging of cells was performed on a Zeiss Observer equipped with a series of objectives and Zen Pro software.

Cell Counting

Cell number quantification was performed using a TC-20 automated cell counter (Biorad) and Trypan Blue (Sigma-Aldrich). Size exclusion was used to isolate the live population of cells between 5 and 20 μm.

Analysis of Flow Cytometry Data

Analysis of flow data was performed using FACSDiva v6.1.3 and FlowJo v10 . All figures were generated with FlowJo. To set the thresholds to specifically detect the cells expressing red-fluorescence, cells expressing either only GFP, or both mCherryFP and

GFP, were used as negative and positive controls. In this study, the detection threshold for signals in the PE-Texas Red channel was set at 5 times of the maximum signal generated by the negative control (10^4 v.s. $2x10^3$). This gate setting is expected to cover more than 70% of true positive cells, as estimated from the distributions of the positive and negative controls in the flow chart (Figures 2A and S2). Provided all samples in an experiment are analyzed with the same criteria and all experimental groups are to be normalized to the same control, this gating threshold may be moved to higher or lower levels to adjust the sensitivity of this assay. This adjustment should be performed by comparing the positive and negative controls as mentioned above to cover sufficient percentage of the positive cells while avoiding the main peak of negative cells. As demonstrated in Figure S4, changing the threshold between $5x10^3$ and $2x10^4$, which corresponds to coverage of the positive cells for about 90% and 60%, respectively, did not generate substantial impacts for the relative signal ratios of the experiment groups when normalized to the controlled group.

QUANTIFICATION AND STATISTICAL ANALYSIS

To Quantify NGS data, transcript counts for different genomic variants were quantified and compared using gVIM v7.3. For the curve fitting with linear regression, the corresponding equation, and coefficient of determination (R^2) were calculated by the built-in function of ''Format Trendline'' in Excel (Microsoft Office Professional Plus, V. 2013). For the statistical analysis, normally distributed data were analyzed for significance by generating P-values from a 2-tailed Student's T-test.

DATA AND SOFTWARE AVAILABILITY

The following data are available in the Mendeley Data depository (https://data.mendeley.com) with this reference number: https://doi.org/10.17632/d56h7fdtjw.1

The DNA sequence and vector construction map for the reporter plasmid pQC-CherryOFF-GFP and the positive control plasmid pQC-mCherryFP-GFP

The NGS data for determining the resolution of the NGS technique (standard curve)

The NGS data for determining the false positive rate in the UV-treated cells that were sorted for red fluorescence.